Improvement in Spacebased Scatterometers and Increased Scientific Impact in the Past Decade

W. Timothy Liu and Xiaosu Xie
Jet Propulsion Laboratory, California Institute of Technology, Pasadena, CA 91109, U.S.A.

ABSTRACT

The past decade has seen continuous improvement to the coverage and resolution of ocean surface winds by spacebased microwave scatterometers. The principles of scatterometry and the characteristics of these sensors are summarized. Examples of scientific applications with these improvements are given. The high quality and resolution of scatterometer winds allow improved study of tropical atmospheric convergence zones, particularly a southern intertropical convergence zone in the Atlantic. Recent scatterometer data describe the wind jets out of Central America with sufficient details to provide the forcing to simulate realistic coastal upwelling in ocean general circulation model. QuikSCAT reveals for the first time an ultra long wake composed of alternate high and low winds streaks and lines of positive and negative curl of wind stress; they stretch a few thousand kilometers from the west side of the Hawaii Islands to beyond Wake Islands in the western Pacific. QuikSCAT also reveal the atmospheric manifestation of the westward-propagating tropical instability waves in the equatorial Pacific. Scatterometers are capable of monitoring not only the ocean winds, which feed moisture towards land, but the consequent flooding of the land. Flooding in Asia, resulting from monsoon and typhoons are described. The plan for future missions and proposed new technology will be presented.

1. PRINCIPLES OF SCATTEROMETRY

During the Second World War, marine radar operators encountered noises on their radar screens, which obscured small boats and low-flying aircraft. They termed the noise "sea clutter". This clutter was the backscatter of the radar pulses by the small waves on the ocean's surface. The radar operators at that time were quite annoyed by these noises, not knowing that a few decades later, important scientific applications are being made from these noises.

The scatterometer sends microwave pulses to the earth's surface and measure the backscattered power from the surface roughness. The roughness may describe characteristics of polar ice or vegetation over land. Over the ocean, which covers over three-quarters of the earth's surface, the backscatter is largely due to the small centimeter waves on the surface. The idea of remote sensing of ocean surface winds was based on the belief that these surface ripples are in equilibrium with the local wind stress. At incident angles greater than 20°, it was confirmed that the backscatter coefficient increases with wind speed [1]. The results also demonstrate the anisotropic characteristics of the scattering. The backscatter depends not only on the magnitude of the wind stress but also the wind direction relative to the direction of the radar beam. The capability of measuring both wind speed and direction is the major uniqueness of the scatterometer. Because the backscatter is symmetric about the mean wind direction, observations at many azimuth angles are needed to resolve the directional ambiguity. The past decade has seen continuous improvement to the coverage and resolution of ocean surface winds.

2. SCATTEROMETER MISSIONS

Historically, scatterometers of the European Space Agency (ESA) used C-band (5 GHz), but the National Aeronautics and Space Administration (NASA) prefers Ku-band (14 GHz). Ku-band is more sensitive to wind variation at low winds but is more subjective to rain contamination. The European Remote Satellite (ERS)-1 and -2 provided nine years of continuous wind data starting 1991, covering 40% of the global ocean daily. The backscatters measured have 50-km spatial resolution but are sampled at 25 km. The NASA Scatterometer (NSCAT) covered 77% of global ocean at 25-km resolution daily. The unexpected destruction of the solar array caused the early demise of NSCAT in June 1997, after returning 9 months of data. NASA launched QuikSCAT in 1999. It covers 93% of the global ocean in a single day. The standard wind product has 25-km spatial resolution, but special products with 12.5-km resolution for selected regions have been produced. Instead of the fan-beam antennas used by all the scatterometer before, QuikSCAT uses pencil-beam antennas in a conical scan and has a continuous 1,800-km swath. In one decade, daily wind vector coverage increases from 41%, to 77%, then to 93%, and spatial resolution improves from 50km, to 25 km, and to 12.5 km.

3. ATMOSPHERIC WIND CONVERGENCE

The high quality and high resolution of scatterometer observations allow better representation of surface wind divergence. Fig. 1a shows the map of wind divergence in boreal winter computed from QuikSCAT data. It clearly identifies the Intertropical Convergence Zone in both the Pacific and the Atlantic, just north of the equator, the South Pacific Convergence Zone, running in an east-southeast direction from New Guinea, and the South Atlantic Convergence Zone, running southeast from Brazil at 20°S. There is a convergence zone parallel to ITCZ, just south of the equator in the eastern Pacific (double ITCZ), but no corresponding features in the Atlantic. These features have been well observed [2]. In boreal summer (Fig. 1), QuikSCAT data reveal a convergence zone running eastward from Brazil at 8°S. Semyon Grodsky (personal communica-

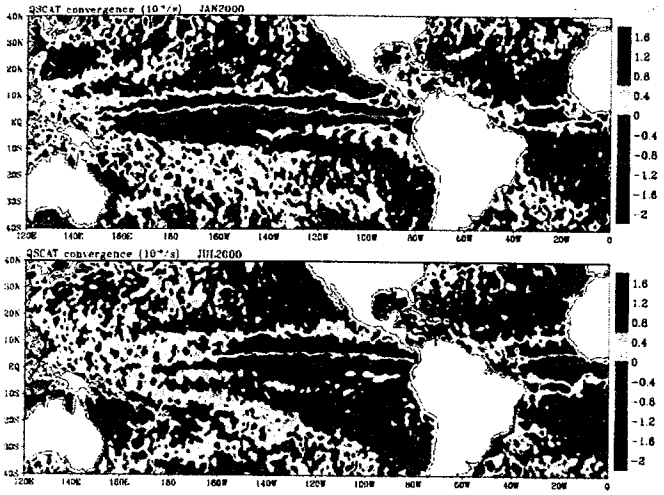

Fig. 1 Ocean surface wind convergence derived from QuikSCAT data for January and July 2000, representing Boreal winter and summer seasons.

tion, 2001) has also observed this convergence zone recently, using the same set of satellite data; otherwise this convergence zone has never been noticed. Fig. 2 shows that the location of wind convergence agrees with belts of high cloud liquid water and high sea surface temperature observed by the microwave radiometer on the Tropical Rain Measuring Mission (TMI) [3]. The seasonal modulation and interannual variation of this convergence zone are being studied.

4. COASTAL WIND JET

Coastal oceans are important to ecology and economy. Coastal upwelling is driven by wind, but wind field with sufficient time and spatial resolution to drive realistic response from ocean model is difficult to find. The wind jets through Central America have received considerable attention recently [4,5]. The chlorophyll concentration observed by the SeaWifs, shown in Fig. 3 reveals ocean upwelling caused by the two wind jets through the mountain gaps of Tehuantepec and Papagayo. SeaWifs is an infrared/visible sensor, which is obscured by clouds. It takes seven days of data to make this map. Most of the time, the wind jets do not last that long. It will take a similar duration to make a map of sea surface temperature (SST) from infrared/visible sensors. Fig. 3 also shows SST from TMI. Because the atmosphere is largely transparent to microwave it takes only two day to make the SST map. Fig. 4 shows one day of standard scatterometer data at 25 km resolution. The detailed wind structure in this daily map provide by spaceborne scatterometer is obvious. For the first time, we have wind field with sufficient details to force an ocean model to reproduce the realistic ocean response. Simulated SST showing area of ocean cooling caused by he wind jets agrees with observations. Cross-sections in the ocean of simulated temperature and vertical velocity show intense upwelling [6].

5. BREAK IN THE TRADES

The Hawaii Islands are the only major obstacles to the steady westward flow of the Trade Winds and North Equatorial Current in the tropical Pacific. According to conventional theories and observations, the wind wakes caused by the islands should dissipate within 300 km downstream, and should not be felt in the western Pacific. The fine resolution of QuikSCAT reveals a persistent wind pattern to the west; composed of alternate high and low winds streaks, and lines of positive and negative curl of wind stress. This pattern stretches a few thousand kilometers from the western side of the Hawaii Islands to beyond Wake Island in the western Pacific. The altimeter of Topex/Poseidon shows, in Fig. 5, bands of positive and negative sea level changes,

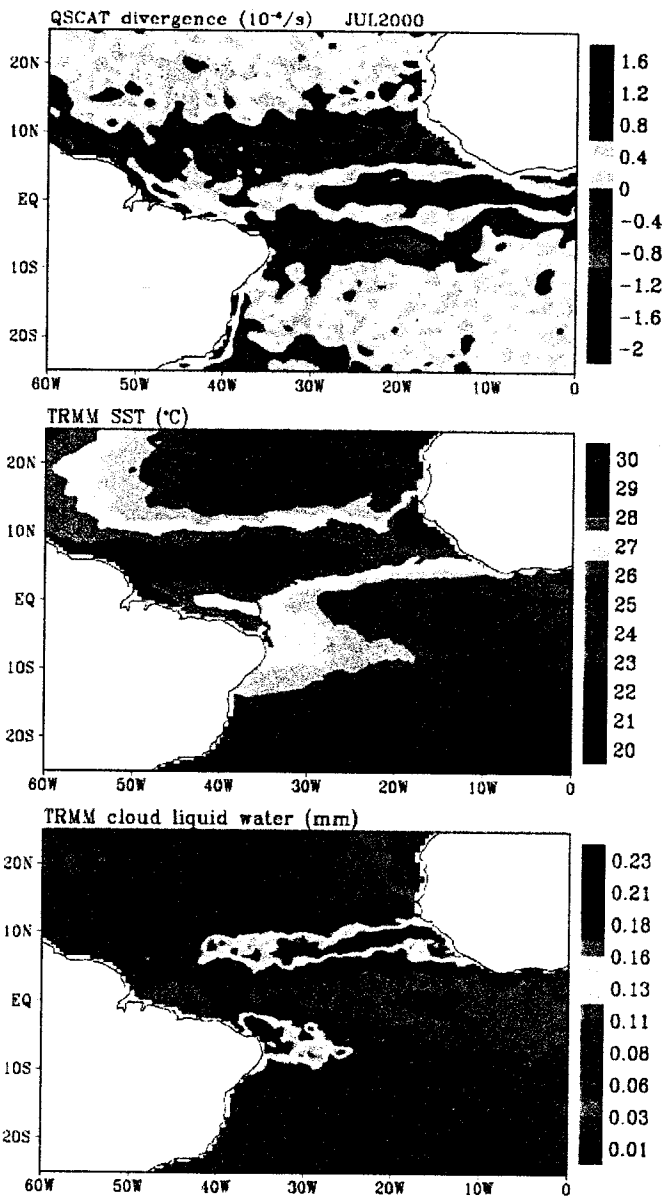

Fig. 2 Surface wind divergence derived form QuikSCAT (upper), sea surface temperature from the microwave imager on TRMM (center), and the cloud liquid water from TRMM, for the month of July 2000 in the tropical Atlantic.

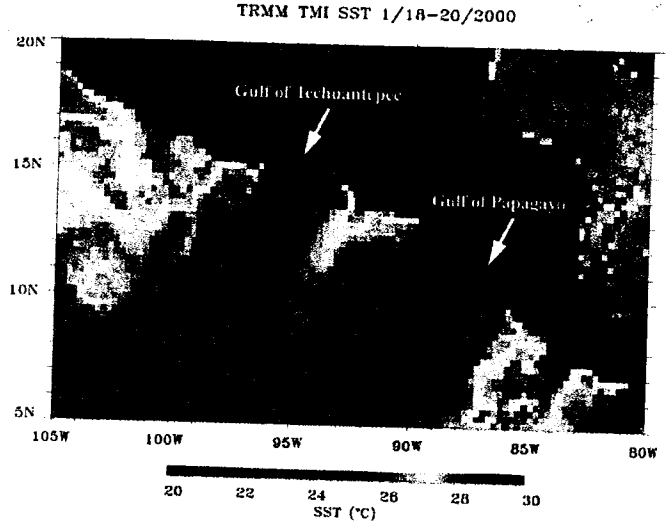

Fig. 3 Three-day average sea surface temperature observed by TMI (upper) and seven-days average chlorophyll concentration observed by SeaWifs in the Gulf of Tehuantepec and Gulf of Papagayo.

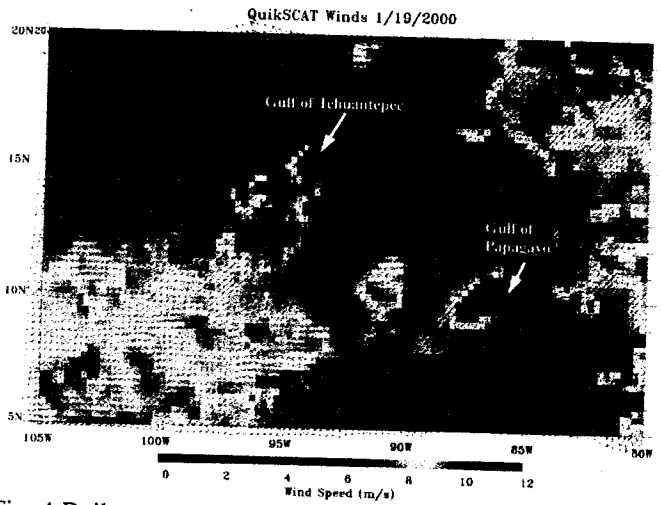

Fig. 4 Daily mean wind vectors superimposed on color image of wind speed derived from QuikSCAT measured by QuikSCAT showing wind jets through Central America.

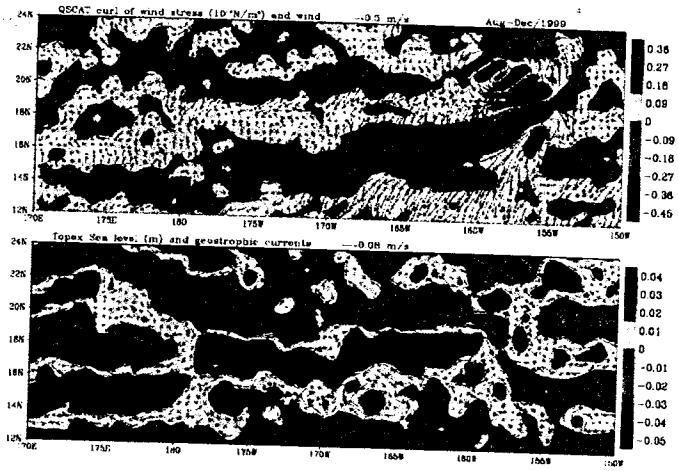

Fig. 5 Ocean surface wind vectors (arrows) superimposed on the curl of wind stress (color image) derived from QuikSCAT (upper). Changes of geostrophic currents (arrows) superimposed on sea level changes derived from Topex/Poseidon (lower). The meridional running-mean representing the large scale gradient has been removed from each set of data.

implying cyclonic and anticyclonic current gyres with an eastward geostrophic current deviation between them at 19°N. TMI reveals a narrow band of warmer water and enhanced atmospheric convection (cloud water) at the position of the geostrophic current deviations, probably resulted from heat advection from the west. QuikSCAT also observes surface wind convergence and vorticity associated with the warm water and convection (Fig. 5). The 'long wake" revealed by QuikSCAT may be sustained by positive feedback between the ocean and the atmosphere. This narrow gap amidst westward flowing wind and current that may have aided the ancient eastward migration of Polynesian across half of the Pacific has never been viewed a single system until QuikSCAT data were combined with two other microwave sensors [7,8].

6. TROPICAL INSTABILITY WAVES

The tropical instability waves (TIW) were best observed as meanders of the temperature front between the cold upwelling water of the Pacific equatorial cold tongue and the warm water to the north. It was first identified by Xie et al. [9] in wind variations observed by the ERS-1 scatterometer. The high quality winds derived from QuikSCAT and coincident all weather SST measurements by TMI reveal the coherent propagation of atmospheric and oceanic parameters associated with TIW. The phase differences infer that the wind-SST coupling is caused by buoyancy instability and mixing in the atmospheric boundary layer, as confirmed by wind profiles measured on a research ship [10]. The analysis was extended to the south of the equator and to the Atlantic Ocean by Hashizume et al. [11]. Data from the scatterometer and the altimeter were also combined to study temperature advection in TIW by Polito et al. [12].

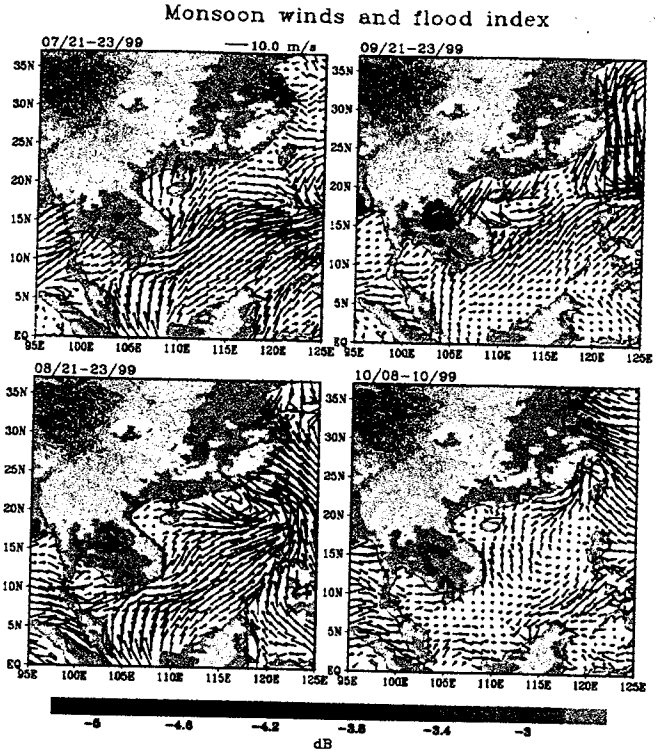

Fig. 6 Three-day average wind vectors over ocean and flood indexes over land derived from QuikSCAT observations, for four months in 1999. Topographic map for areas over 5-m elevation is plotted over flood indexes.

7. FLOOD INDEX

Scatterometers are capable of monitoring not only the ocean winds, which feed moisture towards land, but the consequent flooding of the land. Both scattering and reflection from the surface contribute to the backscatter energy received by the scatterometer. Over dry land, scattering dominates and the horizontal polarization return (H) is smaller than the vertical polarization return (V). When the land gets flooded, however, the reflectivity of the surface increases greatly, and H becomes larger than V. The difference between reflectivity in H and V increases with incident angle, up to 80°. Over flooded land, the ratio in V/H is less than 1 in the linear scale or negative in the dB scale. The opposite is true in the dry case. QuikSCAT measures H at a constant incident angle of 54° over a swath of 1800 km and H at 46° over a 1400-km swath, providing a large difference in reflectivity. It is more conducive to monitor flooding than previous scatterometers, with varying incident angles. QuikSCAT data were used to depict the monsoons and tropical cyclones which brought excessive moisture into the Asian continent and to monitor the subsequent flooding over land, during summer and fall of 1999 [14]. The maps in Fig. 6 show that the flooding in the Yangtze Valley of China (30°N), represented by blue patches, is clearly visible in July, following strong summer monsoons. The flooding observed in Anhui, Zhejiang, and Jiangsu provinces agrees with reports by the International Federation of Red Cross. The flooding recedes in September, with the retreat of the summer monsoon and the advance of the winter monsoon. The intensity of the flooding increases again in October, after the landfall of a typhoon.

8. FUTURE MISSION AND TECHNOLOGY

Quikscat will be followed by an identical scatterometer on ADEOS-2 scheduled to be launched in February 2002. If there is sufficient overlap between the operations of the two identical scatterometers, the importance of high-frequency wind forcing on the ocean can be demonstrated [Milliff et al., 2001]. ESA is planning to launch a series of C-band dual-swath advance scatteroemter (ASCAT), on their operational platform METOP, starting in December 1995. NASA is planning to launch a polarimetric scatterometer on the Japanese Global Change Observation Mission (GCOM), so that two wide-swath scatterometers will provide continuous time series of high frequency wind forcing.

One of the drawbacks on scatterometer is the wind-direction ambiguity. The backscatter is a cosine function of the azimuth angle (angle between radar beam and wind direction). In a recent experiment, it was demonstrated the correlation between copolarized and cross-polarized backscatter is a sine function of azimuth angle. By adding receiver of cross polarized backscatter to the scatterometer on QuikSCAT, the directional ambiguity problem can be eliminated [13]. Although QuikSCAT has a continuous scan, the azimuth angles are too close together at the outer swath and too far apart near nadir, hampering selection of wind direction. With polarimetric scatterometer, we can achieve uniform retrieval accuracy across the entire swath. Polarimetric scatterometer can separate rain effect in the atmosphere from that at the surface, and perhaps can improve the accuracy of retrieving wind under rain. Polarimetric scatterometer does not require full circular scan to get the azimuth angles, and will ease accommodation problem on spacecraft. We strive to infuse new technology to extend applications and to ease transition into operational spacecraft, while preserving the continuity of high quality wind-vector measurements.

9. DATA AVAILABILITY

Twice-daily maps of surface winds over global oceans, derived from objective interpolation of the observations by QuikSCAT are displayed at http://airsea-www.jpl.nasa.gov. Digital data can be downloaded on line. Near-real-time scatterometer winds maps in swath format are displayed at http://manati.wwb.noaa.gov/quikscat. Standard NSCAT and QuikSCAT data can be requested through http://podaac.jpl.nasa.gov.

ACKNOWLEDGMENT

This study was performed at the Jet Propulsion Laboratory, under contract with the National Aeronautics and Space Administration (NASA). It was supported by the

Physical Oceanography and Ocean Vector Wind Programs of NASA.

REFERENCES

[1] Jones, W.L., F.J. Wentz, and L.C. Schroeder, "Algorithm for inferring wind stress from SEASAT-A", J. Spacecraft and Rockets, 15, 368-374, 1978.

[2] Zheng, Q., X.H. Yan, W.T. Liu, W. Tang, and D. Kurz, "Seasonal and interannual variability of atmospheric convergence zones in the tropical Pacific observed with ERS-1 scatterometer", Geophys. Res. Lett., 24, 261-263, 1977.

[3] Liu, W.T., "Progress in scatterometer application:, J. Oceanogr., in press, 2001

[4] Bourassa, M., L. Zamudio, and J.J. O'Brien, "Noninertial flow in NSCAT observations of Tehuantepec winds", J. Geophy. Res., 104, 11,311-11,319, 1999.

[5] Chelton, D.B., M.H. Freilich, and S.K. Esbensen, "Satellite observations of the wind jets off the Pacific coast of Central America." Part I: Case studies and statistical characteristics. Mon. Wea. Rev., 128, 1993-2018, 2001

[6] Liu, W.T., H. Hu, Y.T. Song, and W. Tang, "Improvement of scatterometer wind vectors - impact on hurricane and coastal studies", Proc. WCRP/SCOR Workshop of Airsea Flux Validation, World Climate Research Programme, Geneva, in press, 2001

[7] Liu, W.T., "Wind over troubled water", Backscatter, 12, No. 2, 10-14, 2001.

[8] Xie, S.P., W. T. Liu, and Q. Liu, and M. Nonaka, "Far-reaching effects of the Hawaiian Island on the Pacific Ocean-Atmosphere", Science, 292.2057-2060, 2001.

[9] Xie, S.P., M. Ishiwagtari, H. Hashimsum, and K.Takeuchi, "Coupled ocean-atmosphere waves on the equatorial front", Geophys. Res. Lett., 25, 3863-2966, 1998.

[10] Liu, W.T., X. Xie, P.S. Polito, S. Xie, and H. Hashizume, "Atmosphere manifestation of tropical instability waves observed by QuikSCAT and Tropical Rain Measuring Missions', Geophys. Res. Lett., 27, 2545-2548, 2000.

[11] Hashizume, H., S-P Xie, W.T. Liu, and K. Takeuchi, "Local and remote atmospheric response to tropical instability waves: a global view from space.', J. Geophys. Res., 106, 10173-10185, 2001.

[12] Polito, P., J.P. Ryan, W.T. Liu, and F.P. Chavez, "Oceanic and Atmospheric Anomalies of Tropical instability Waves', Geophys. Res. Lett., 28, 2233-2236, 2001.

[13] Tsai, W.-Y., S. Nghiem, J. Huddelstgon, M. Spencer, B. Stiles and R. West, "Polarimetric scatterometer: a promising technique for improving ocean surface measurements from space", IEEE trans. Geosci. Remote Sensing, 38, 1903-1921, 2000.

[14] Liu, W.T., X. Xie, W. Tang, and S.V. Nghiem, 2001b: Wind Changes over the Western Pacific. East Asia and Western Pacific Meteorology and Climate. Vol. 4, World Scientific Co., London. in press.